Accepted for publication in *The Astrophysical Journal*

Optical Spectral Variability of the Very-High-Energy Gamma-Ray Blazar 1ES 1011+496

M. Böttcher[1], B. Hivick[1], J. Dashti[1], K. Fultz[1], S. Gupta[1], C. Gusbar[1], M. Joshi[1,2], A. Lamerato[1], T. Peery[1], D. Principe[1,3], A. Rajasingam[1], P. Roustazadeh[1], J. Shields[1]

ABSTRACT

We present results of five years of optical (UBVRI) observations of the very-high-energy gamma-ray blazar 1ES 1011+496 at the MDM Observatory. We calibrated UBVRI magnitudes of five comparison stars in the field of the object. Most of our observations were done during moderately faint states of 1ES 1011+496 with $R \gtrsim 15.0$. The light curves exhibit moderate, closely correlated variability in all optical wavebands on time scales of a few days. A cross-correlation analysis between optical bands does not show significant evidence for time lags. We find a positive correlation (Pearson's $r = 0.57$; probability of non-correlation $P(> r) \approx 4 \times 10^{-8}$) between the R-band magnitude and the B - R color index, indicating a bluer-when-brighter trend. Snap-shot optical spectral energy distributions (SEDs) exhibit a peak within the optical regime, typically between the V and B bands. We find a strong ($r = 0.78$; probability of non-correlation $P(> r) \approx 10^{-15}$) positive correlation between the νF_ν peak flux and the peak frequency, best fit by a relation $\nu F_\nu^{\rm pk} \propto \nu_{\rm pk}^k$ with $k = 2.05 \pm 0.17$. Such a correlation is consistent with the optical (synchrotron) variability of 1ES 1011+496 being primarily driven by changes in the magnetic field.

Subject headings: galaxies: active — BL Lacertae objects: individual (1ES 1011+496) — radiation mechanisms: non-thermal

[1]Astrophysical Institute, Department of Physics and Astronomy, Clippinger 251B, Ohio University, Athens, OH 45701, USA

[2]Institute for Astrophysical Research, Boston University, 725 Commonwealth Ave., Boston, MA 02215, USA

[3]Rochester Institute of Technology, 84 Lomb Memorial Drive, Rochester, NY 14623, USA

1. Introduction

Blazars are the most violent class of active galactic nuclei, consisting of flat-spectrum radio quasars (FSRQs) and BL Lac objects (named after their historical prototype, BL Lacertae). They exhibit rapid variability down to time scales as short as a few minutes (Aharonian et al. 2007; Albert et al. 2007a). Their observed flux is dominated by a non-thermal continuum exhibiting two broad spectral bumps: A low-frequency bump from radio to UV – X-ray frequencies, and a high-frequency component from X-ray to γ-rays. In the framework of relativistic jet models, the low-frequency (radio – optical/UV) emission from blazars is interpreted as synchrotron emission from nonthermal electrons in a relativistic jet. The high-frequency (X-ray – γ-ray) emission could either be produced via Compton upscattering of low frequency radiation by the same electrons responsible for the synchrotron emission (leptonic jet models; for a recent review see, e.g., Böttcher 2007), or due to hadronic processes initiated by relativistic protons co-accelerated with the electrons (hadronic models, for a recent discussion see, e.g., Mücke & Protheroe 2001; Mücke et al. 2003).

To date, about 30 blazars have been detected in very high energy (VHE, > 100 GeV) γ-rays with ground-based air Čerenkov telescope facilities[1]. Most of these TeV blazars belong to the sub-class of high-frequency peaked BL Lac objects (HBLs). They are characterized by a synchrotron spectrum peaking at frequencies $\nu_{\rm sy}^{\rm pk} \gtrsim 10^{15}$ Hz, i.e., in the UV or X-ray range, and γ-ray peaks at $\nu_{\gamma}^{\rm pk} \gtrsim 10^{25}$ Hz, i.e., typically beyond the Fermi energy range (Abdo et al. 2010). VHE γ-rays from sources at cosmological distances can be absorbed by the extragalactic background light (EBL) due to $\gamma\gamma$ pair production (e.g., Dwek & Krennrich 2005; Stecker et al. 2006; Franceschini et al. 2008; Gilmore et al. 2009; Finke et al. 2010). Hence, the EBL absorption of distant VHE γ-ray sources may provide a probe of the spectrum and cosmological evolution of the EBL, which is notoriously difficult to measure directly due to bright foregrounds.

The BL Lac object 1ES 1011+496 was detected as a VHE γ-ray emitter by MAGIC in the spring of 2007 (Albert et al. 2007b). Follow-up optical spectroscopy at the MMT confirmed the previously uncertain redshift of $z = 0.212 \pm 0.002$ for this source (Albert et al. 2007b). At the time of its VHE detection, 1ES 1011+496 was the most distant VHE γ-ray source known with a well-determined redshift, and to date it still ranks among the top five. It might therefore offer a prime opportunity for studying the EBL through its absorption signature at VHE γ-rays. However, in order to exploit this opportunity, a thorough understanding of the intrinsic spectral energy distribution (SED) of the source, constrained through observations at lower (radio through GeV γ-ray) frequencies, is essential. For this purpose, we present

[1]For a complete list of VHE γ-ray sources see `http://tevcat.uchicago.edu`

here a detailed study of the optical spectral variability of this object with data gathered over the course of 5 years at the 1.3m McGraw-Hill Telescope of the MDM Observatory on Kitt Peak, Arizona.

The VHE γ-ray detection of 1ES 1011+496 was triggered by a large optical outburst of the source in 2007 March (Albert et al. 2007b). This object is regularly monitored in the optical R-band through the Turku blazar monitoring program led by Kari Nilsson, with the 1.03 m telescope of the Tuorla Observatory in Finland, as well as the 35 cm telescope of the KVA Observatory on La Palma, Canary Islands, Spain[2]. Apart from this, 1ES 1011+496 has so far received rather little attention by optical observers, and its optical spectral variability has remained unexplored. The object has been observed in X-rays by Einstein (Elvis et al. 1992) and more recently, Swift/XRT (Abdo et al. 2010). In all observations, it shows a steep X-ray spectrum, indicating the dominance of synchrotron emission in the X-ray regime. 1ES 1011+496 may also be associated with the EGRET γ-ray source 3EG J1009+4855 (Hartman et al. 1999), although this association is uncertain (Sowards-Emmerd et al. 2003). The object is clearly detected by Fermi and listed in the Fermi 3-month catalogue as the source 0FGL J1015.2+4927. The Fermi data reveal a rising νF_ν spectrum (i.e., photon index $\Gamma < 2$) in the 100 MeV – 30 GeV energy range (Abdo et al. 2010).

Optical/UV observations were performed by Swift/UVOT in May 2008 (Abdo et al. 2010), during the rising phase of an optical outburst similar to the one triggering the MAGIC discovery observations in 2007. During those observations, Swift/UVOT measured a rising νF_ν optical/UV continuum spectrum. This, together with the hard Fermi spectrum, justified the classification of 1ES 1011+496 as an HBL.

Over the course of ~ 5 years, we have collected optical multi-band (UBVRI) photometric data on 1ES 1011+496. As there are no comparison stars with reliably calibrated UBVRI magnitudes in the field of view of this object, we calibrated the magnitudes for 5 comparison stars. In §2 we describe the observations, data reduction, the calibration of comparison-star magnitudes, as well as general features of the light curves. Results of a spectral-variability study are presented in §3. We performed a cross-correlation analysis between the variability patterns in different optical bands, which we describe in §4. We summarize and discuss our results in §5.

[2]Daily light curves are posted at `http://users.utu.fi/kani/1m/index.html`

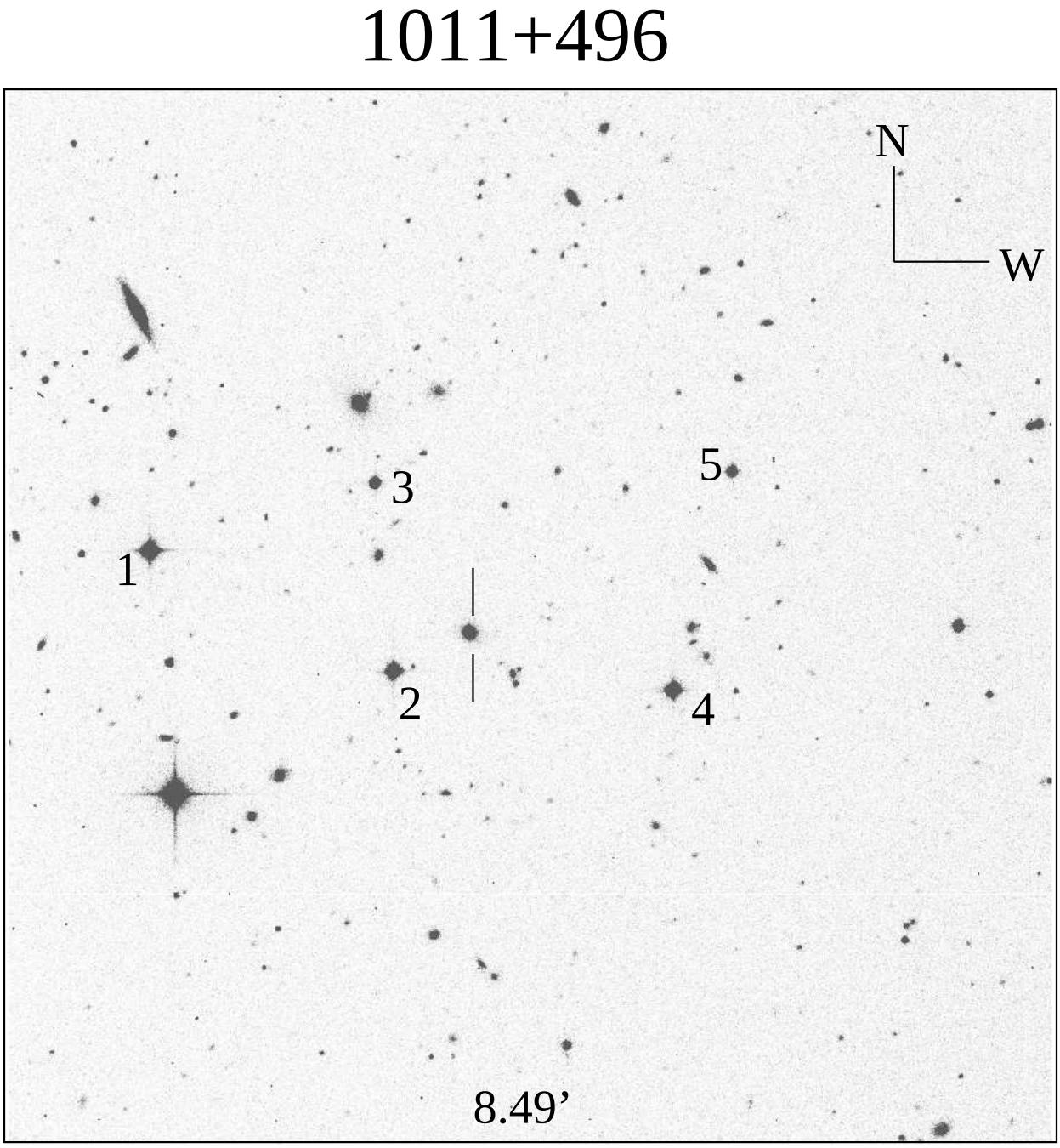

Fig. 1.— Finding chart (R band) of the field around 1ES 1011+496 with 5 comparison stars

2. Observations, data reduction, and light curves

Optical (UBVRI) data were collected at the 1.3m McGraw-Hill Telescope of the MDM Observatory on the south-west ridge of Kitt Peak, Arizona, during 9 $\sim$ 1-week observing runs in 2005 April, September, and December, 2008 April and May, 2009 February and May, and 2010 April and July. The telescope is equipped with standard Johnson-Cousins UBVRI filters. Exposure times for science frames on 1ES 1011+496 were between 60 – 180 s, depending on filter and atmospheric conditions. All frames were bias-subtracted and flat-field corrected using standard routines in IRAF.

In order to be able to perform relative photometry with comparison stars in the field of view, well-calibrated UBVRI magnitudes of those stars need to be known. Since no such information is currently available in the literature, we calibrated UBVRI magnitudes of five comparison stars in the field of view, as indicated in Fig. 1. For the calibration, we obtained a total of 30 (2 per filter per standard) exposures of the Landoldt Equatorial standards (Landoldt 1992) PG 1525-071, PG 1633+099, PG 1657+078 on the night of April 28, 2005, which provided photometric observing conditions. Instrumental magnitudes of these three Equatorial standards as well as our comparison stars in the field of 1ES 1011+496 were extracted using the *phot* routine within the IRAF package DAOPHOT. Following standard procedures for IRAF photometric calibrations (Massey & Davis 1992), we used the routine *fitparams* to solve the transformation equations to evaluate the calibrated, physical magnitudes of our standard stars. The resulting calibrated magnitudes are listed in Table 1.

After calibration of our comparison stars, we extracted instrumental magnitudes of the comparison stars and 1ES 1011+496 using the *phot* routine within the DAOPHOT package of IRAF, and converted instrumental to physical magnitudes assuming that the difference between instrumental and physical magnitudes is the same for the object and all comparison stars. The resulting light curves for all observing runs combined are displayed in Fig. 2. The figure illustrates that for most of our runs, the object was in a rather faint optical state with $R \gtrsim 15.0$, and shows very moderate variability.

Table 1. Calibrated Magnitudes of Comparison Stars in Fig. 1

Star	U	B	V	R	I
1	15.355 ± 0.010	14.738 ± 0.002	13.885 ± 0.002	13.493 ± 0.002	12.973 ± 0.003
2	15.230 ± 0.050	15.109 ± 0.003	14.447 ± 0.002	14.069 ± 0.002	13.703 ± 0.003
3	17.456 ± 0.043	16.788 ± 0.007	15.918 ± 0.003	15.437 ± 0.005	15.013 ± 0.007
4	14.488 ± 0.018	14.698 ± 0.002	14.334 ± 0.002	14.067 ± 0.002	13.797 ± 0.003
5	16.477 ± 0.018	16.539 ± 0.008	15.794 ± 0.003	15.448 ± 0.005	15.125 ± 0.008

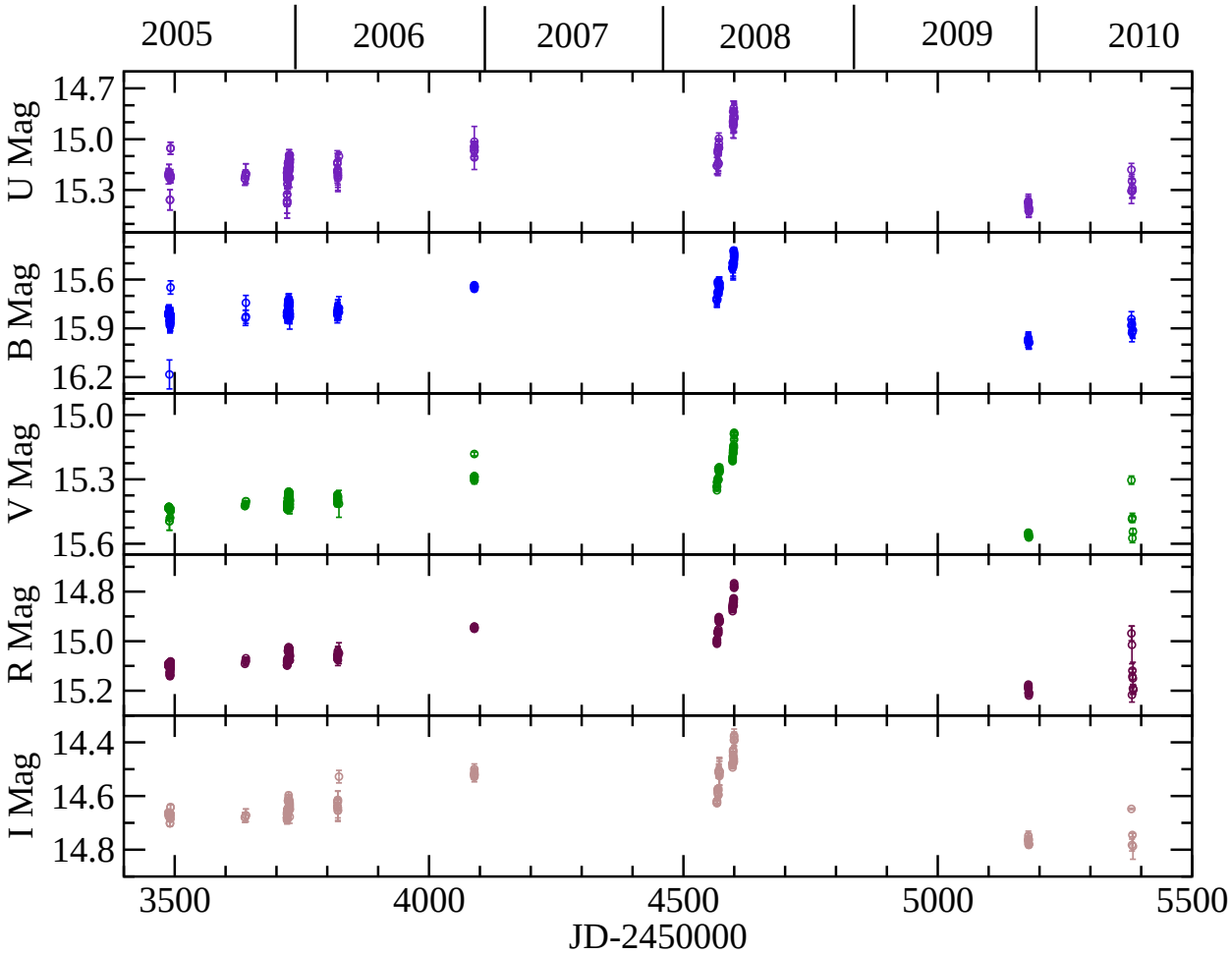

Fig. 2.— Multi-band (UBVRI) light curves of 1ES 1011+496 from our MDM observations

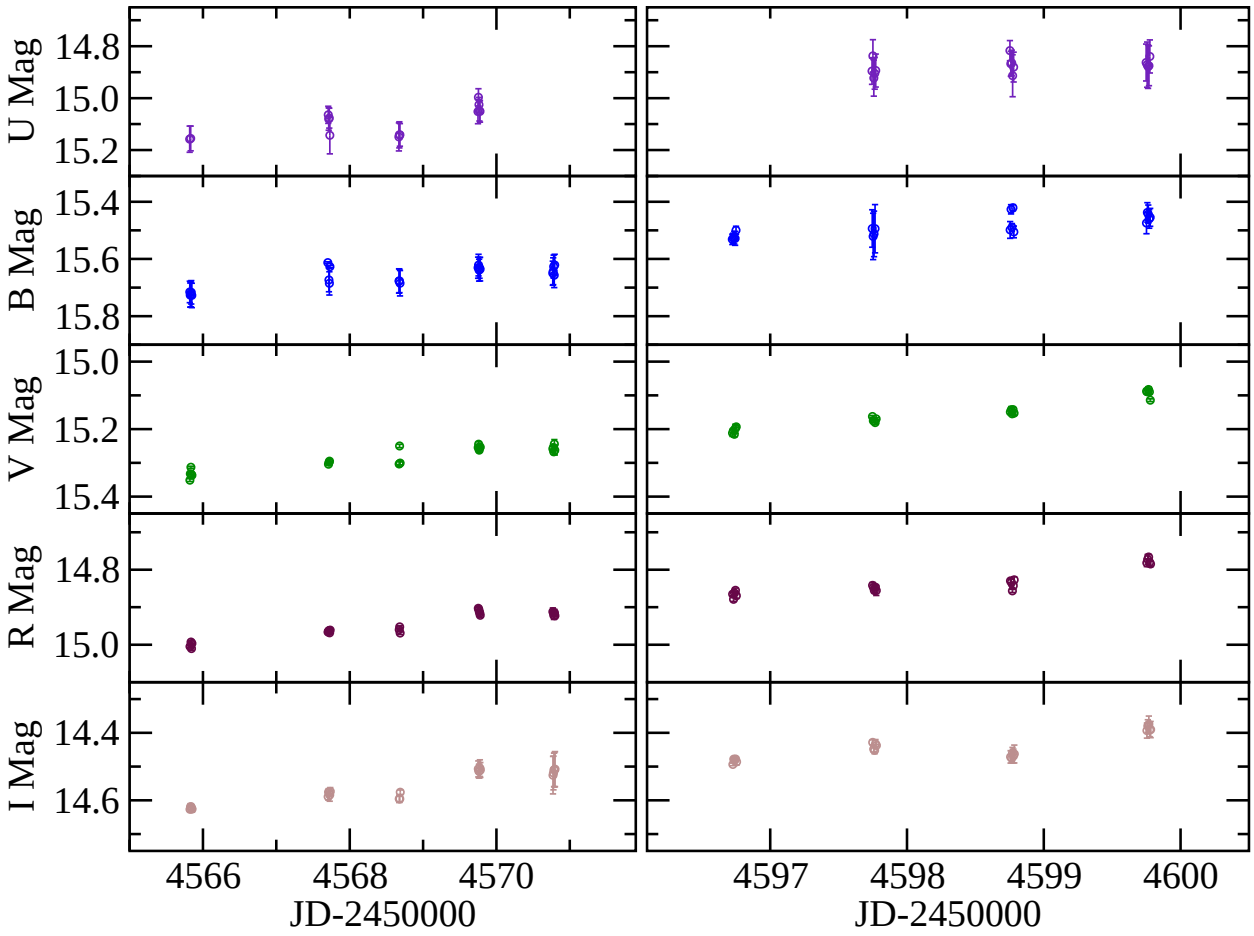

Fig. 3.— Multi-band (UBVRI) light curves of 1ES 1011+496 during the high activity state in April – May 2008

However, we did observe substantial variability during our two observing runs in 2008 April 9 – 14 and May 10 – 13. This was during the rising phase of a major outburst that peaked later that year. Unfortunately, to our knowledge, there are no observations available covering the peak of that outburst. During our observations we found a maximum R-band brightness of $R \sim 14.8$. The object later exceeded $R_{\rm peak} < 14.6$[3]. Fig. 3 shows the multi-band light curves from our 2008 April and May runs. They exhibit variability on time scales of a few days, but no evidence for intraday variability. The variability in all optical bands appears well correlated. This correlation will be investigated in more detail in §4.

3. Optical spectral variability

In order to test whether the variability discussed in the previous section is associated with spectral changes, we first calculated B - R color indices for any pair of B and R magnitudes measured within 15 minutes of each other. The resulting color-magnitude diagram (R magnitude vs. B - R color) is shown in Figure 4. Error bars on B - R are calculated via standard error progatation, i.e., $\sigma_{B-R} = \sqrt{\sigma_R^2 + \sigma_B^2}$. The data clearly indicate color variability. A fit of a constant B - R color as a function of R magnitude results in $\chi^2_\nu = 2.86$. A fit of a linear correlation results in a marginally acceptable $\chi^2_\nu = 1.36$. A correlation analysis of the color-magnitude data set yields a Pearson's correlation coefficient of $r = 0.57$, which is generally interpreted as a weak positive correlation between color and magnitude. In order to quantify the probability of such a correlation coefficient resulting from an uncorrelated data set, we performed Monte-Carlo simulations of 1 billion randomly produced, uncorrelated data sets, extending over similar spreads of values, and with the same number of data points as our observational data set. The Pearson's correlation coefficient for each set was evaluated, and from the entire ensemble, the probability of a correlation coefficient $|r| > x$ for values of $0 < x < 1$ resulting from an uncorrelated data set was evaluated. From these simulations, we find that the probability of a correlation coefficient of $r = 0.57$ in a data set with the characteristics of our R vs. B - R data is $P(|r| \geq 0.57) \approx 4 \times 10^{-9}$, indicating, in fact, a highly significant correlation. The observed correlation corresponds to a bluer-when-brighter trend, as observed in most BL Lac objects. This is likely to reflect the dynamics of the non-thermal synchrotron emission from the jet dominating in the optical regime.

In order to investigate spectral changes in the optical continuum in more detail, we extracted UBVRI SEDs for all sequences of magnitudes measured within 15 minutes of each other. For this purpose, the magnitudes were de-reddened using the Galactic extinction

[3] `http://users.utu.fi/kani/1m/index.html`

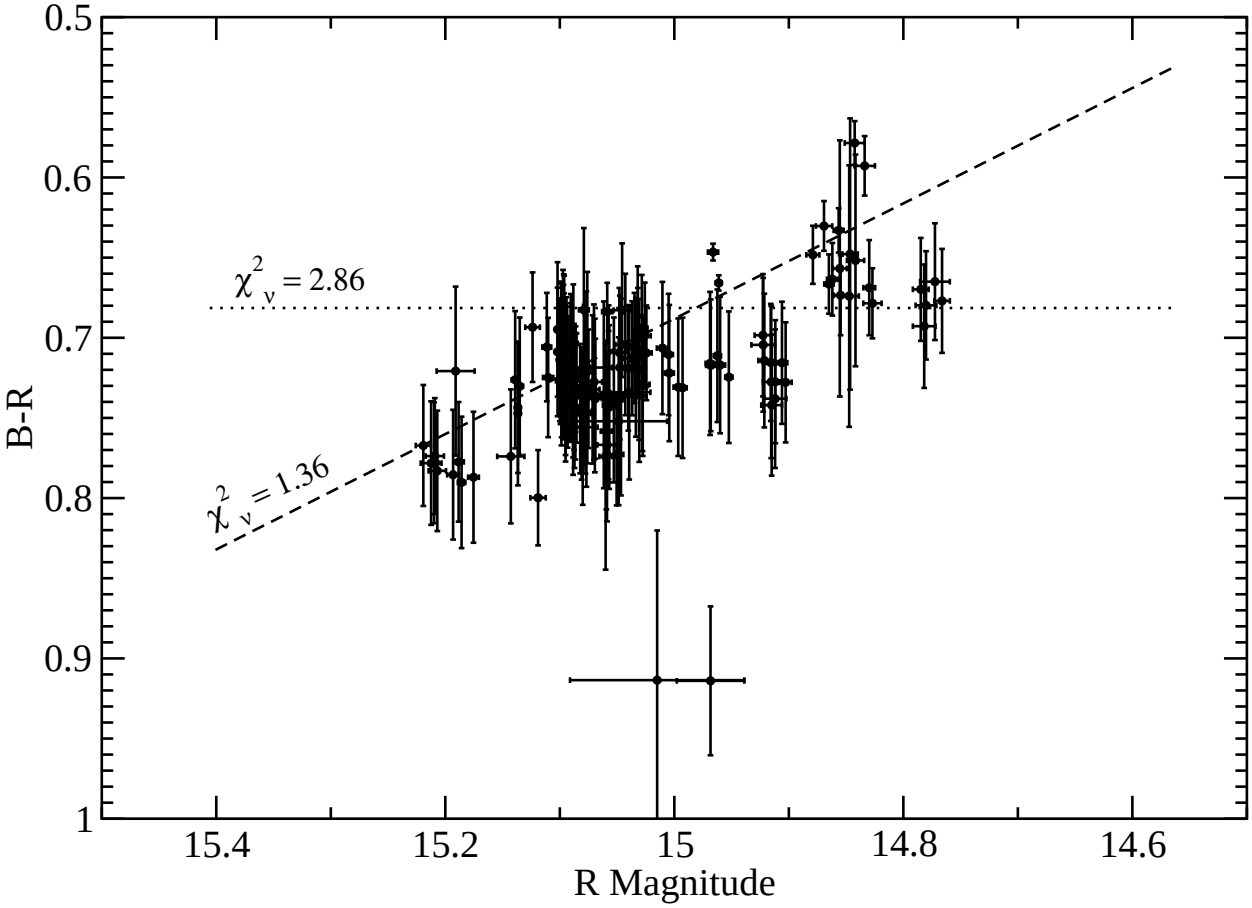

Fig. 4.— Color-magnitude diagram for 1ES 1011+496. The data show significant color variability. A positive linear correlation (bluer when brighter) is indicated by a Pearson's correlation coefficient of $r = 0.57$, with a probability for non-correlation of $P(> r) \approx 4{\times}10^{-9}$.

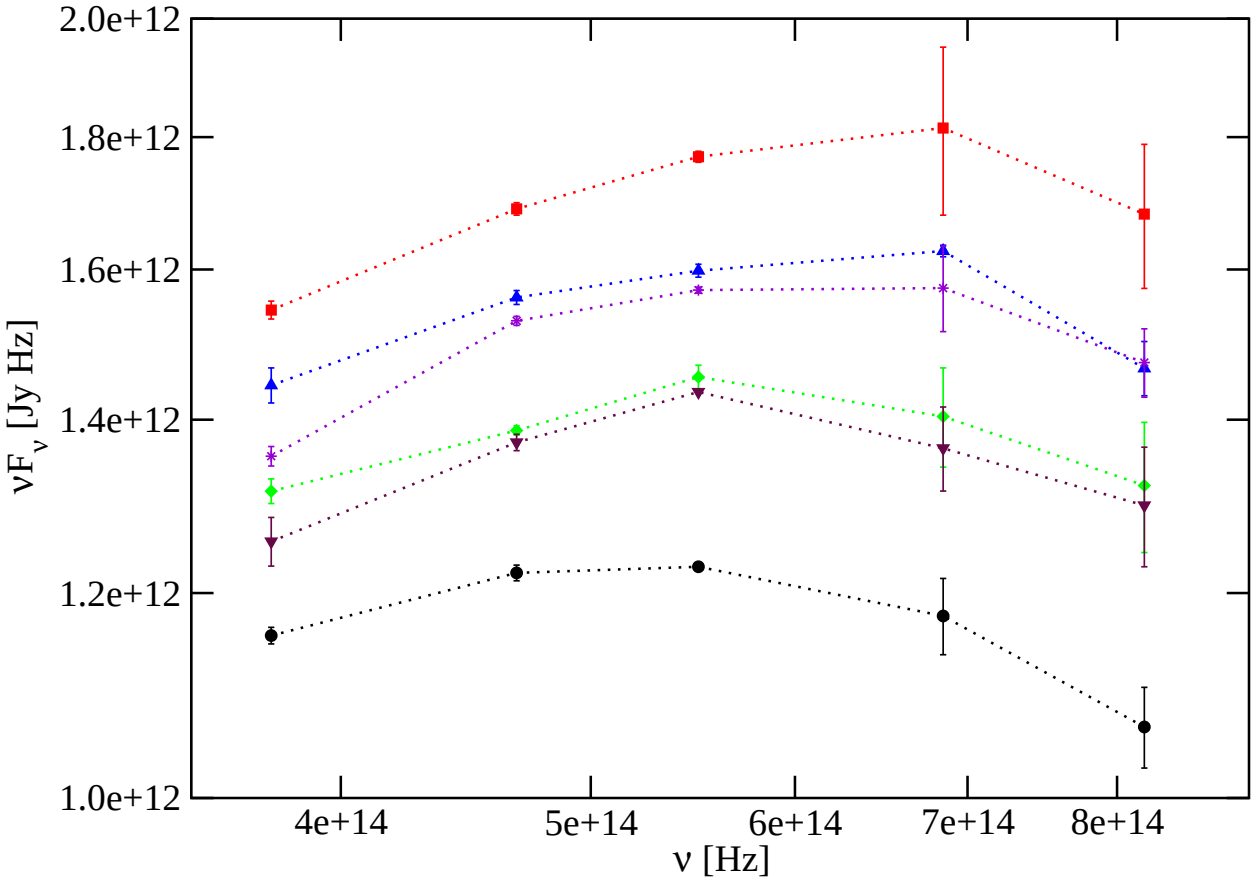

Fig. 5.— Snap-shot UBVRI SEDs of 1ES 1011+496. The SEDs reveal a νF_ν peak typically between the B and V band and suggest a positive correlation between νF_ν peak flux and peak frequency.

coefficients as given in the NASA Extragalactic Database[4] and converted to νF_ν fluxes. A representative sample of the resulting SEDs is plotted in Figure 5. The SEDs all exhibit a νF_ν peak in the optical regime, typically between the V and B bands. They suggest a positive trend of increasing νF_ν peak flux with increasing peak frequency, in accordance with the weak B - R vs. R correlation found above. We tested this hypothesis further by fitting all optical SEDs with a simple parabolic shape to determine the peak frequency, $\nu_{\rm peak}$, and the peak flux, $\nu F_\nu^{\rm pk}$. The best fit values for our entire data set are plotted in Fig. 6.

The νF_ν peak flux and peak frequencies are clearly correlated, with Pearson's $r = 0.78$, with a probability for non-correlation of $P(> r) \approx 10^{-15}$. The best linear regression fit to the logarithms of the $\nu F_\nu^{\rm pk}$ and $\nu_{\rm pk}$ values yields a power-law correlation $\nu F_\nu^{\rm pk} \propto \nu_{\rm pk}^k$ with $k = 2.05 \pm 0.17$. A possible interpretation of this synchrotron peak shift will be discussed in §5.

A visual inspection of Figure 6 seems to suggest a steepening of the peak flux vs. peak frequency dependence towards high peak frequencies (and peak fluxes). However, when restricting the regression to high frequencies (e.g., $\nu_{\rm pk} \gtrsim 6.2 \times 10^{14}$ Hz), the correlation between peak flux and peak frequency vanishes, therefore not allowing for a quantification of a possible change of the correlation slope towards high frequencies.

4. Cross-correlation analysis

A visual inspection of the light curves in Fig. 2 and 3 suggests that the variability in all wavebands is closely correlated. In order to corroborate this finding, we performed a Discrete Correlation Function (DCF, Edelson & Krolik 1988) analysis among all our light curves. Figure 7 shows a typical example of the resulting DCF between the B and R band light curves. The DCFs between the light curves of all bands peak at values near 1, indicating a close correlation between all optical bands. This is expected if the optical continuum is dominated by nonthermal synchrotron emission of the same relativistic electron population. Time lags between different frequency bands could potentially serve as a diagnostic of the magnetic field strength in the emitting region (modulo the Doppler factor, see, e.g., Böttcher 2007). We therefore fitted the DCFs with an asymmetric Gaussian to determine possible inter-band delays through the fitted peak of the DCF. However, any lags indicated by our DCFs are all either consistent with 0 or at the $\sim 1 - 2\ \sigma$ level. Furthermore, our sequential data-taking process introduces an artificial "lag" of up to ~ 10 min, and none of the lags found through the DCF analysis are larger than that. Therefore, we conclude that we did

[4] `http://nedwww.ipac.caltech.edu/`

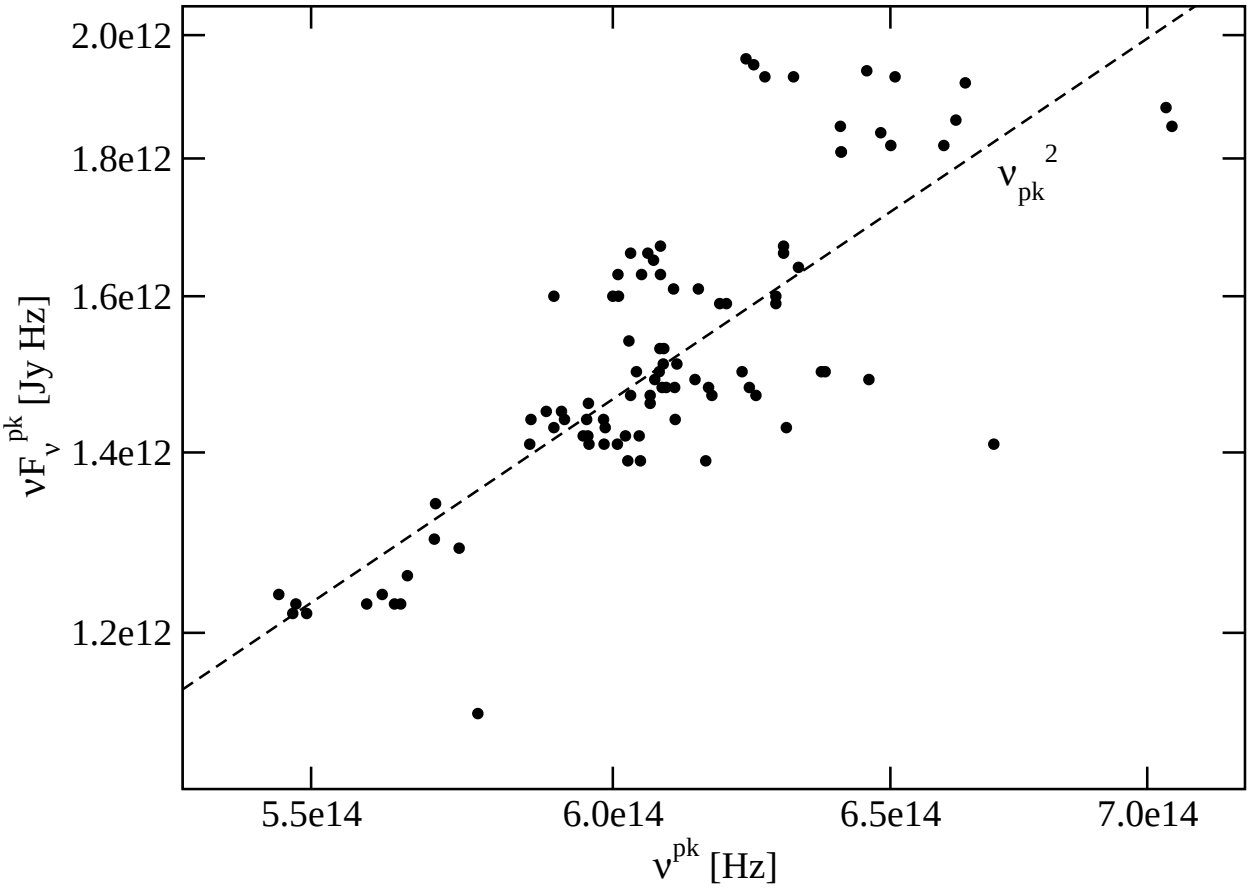

Fig. 6.— Best-fit peak frequency vs. peak νF_ν flux for the entire data set. The data show a significant correlation ($r = 0.78$, $P(> r) \approx 10^{-15}$), best fit by a dependence $\nu F_\nu^{\rm pk} \propto \nu_{\rm pk}^k$ with $k = 2.05 \pm 0.17$. The dashed line indicates a putative correlation with index $k = 2$.

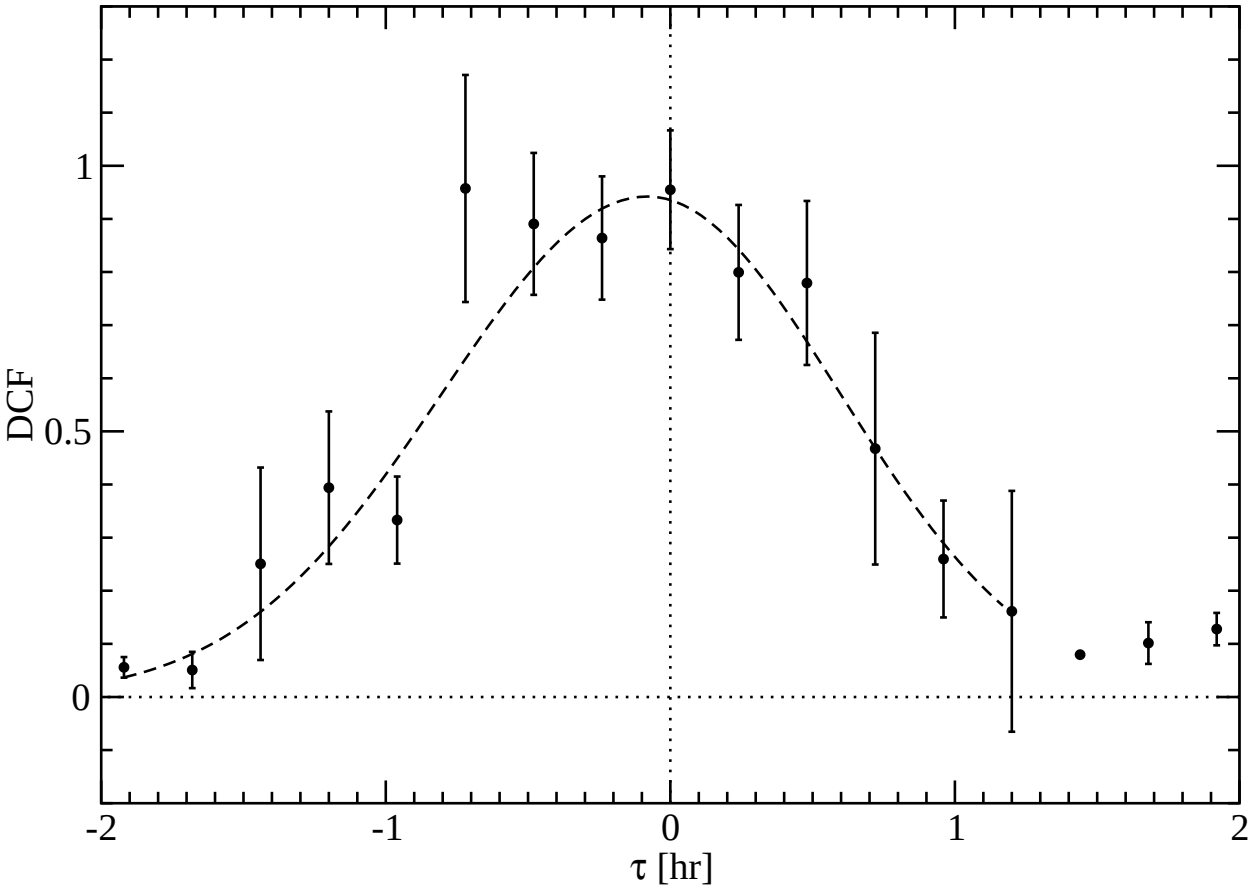

Fig. 7.— Discrete Correlation Function between the B and R bands. A positive τ would indicate a hard lag. The DCF has been fitted with an asymmetric Gaussian. The best-fit peak delay is $\tau_{\rm pk} = (-4.8 \pm 3.2)$ min.

not detect any inter-band time lags.

5. Summary and Discussion

We have presented an analysis of data from 5 years of observations of the BL Lac object 1ES 1011+496 at the 1.3m McGraw-Hill Telescope of the MDM Observatory. We found moderate variability on a time scale of several days throughout most of our observations. The variability at all (UBVRI) optical bands is well correlated with no detectable time lags between them. The snap-shot SEDs during our observations showed a synchrotron peak within the optical range, typically between the V and B bands. The B - R color is correlated ($r = 0.57$; $P_{\rm uncorr}(> r) \approx 4 \times 10^{-8}$) with the R-band magnitude, indicating a bluer-when-brighter trend. Such a trend is observed in many BL Lac objects, where the optical emission is strongly dominated by synchrotron emission from the jet. We note that the opposite behaviour has been found in several quasar-type blazars, where a slowly variable Big Blue Bump, signaling a contribution due to a luminous accretion disk, dilutes the continuum variability at the blue end of the optical spectrum (e.g., Raiteri et al. 2008).

An analysis of the location of the synchrotron peak within the optical regime reveals a peak shift characterized by $\nu F_\nu^{\rm pk} \propto \nu_{\rm pk}^k$ with $k = 2.05 \pm 0.17$, consistent with a $\nu_{\rm pk}^2$ scaling.

There is a range of possible causes for the optical (and multi-wavelength) variability of blazar emission. These include changes in the Doppler factor (e.g., caused by a bending jet), injection of a new relativistic particle population into the jet (plausibly caused by a shock), a changing acceleration efficiency (changing characteristic Lorentz factors of the radiating electrons and possibly a change of the spectral index of the non-thermal electron distribution), and/or a change of the magnetic field. In a realistic scenario, several of these effects might be at work at the same time to produce the observed blazar variability. However, one can make simple predictions concerning the shift (in frequency and νF_ν peak flux) of the synchrotron peak for at least three cases: A changing Doppler factor, a changing magnetic field, and a change of the characteristic (peak) electron Lorentz factor (leaving all other parameters of the emission region unchanged).

The peak frequency of the synchrotron spectrum is related to a peak in the electron spectrum at a characteristic Lorentz factor γ_p, the magnetic field B and the Doppler factor $D = (\Gamma\,[1 - \beta_\Gamma \cos\theta_{\rm obs}])^{-1}$, where $\Gamma = (1 - \beta_\Gamma^2)^{-1/2}$ is the bulk Lorentz factor of the emission region and $\theta_{\rm obs}$ is the angle between the line of sight towards Earth and the direction of motion (the jet axis), through

$$\nu_{\rm pk} \propto \gamma_p^2 \, B \, D \tag{1}$$

The νF_ν flux at the synchrotron peak is related to those quantities through

$$\nu F_\nu^{\rm pk} \propto \gamma_p^2 \, B^2 \, D^4 \tag{2}$$

From equations 1 and 2, we see that if the variability is dominated by a changing Doppler factor, one would expect a synchrotron peak shift as $\nu F_\nu^{\rm pk} \propto \nu_{\rm pk}^4$. A change solely in the characteristic electron Lorentz factor, γ_p, would result in a synchrotron peak shift as $\nu F_\nu^{\rm pk} \propto \nu_{\rm pk}$, while a change in only the magnetic field yields the behaviour $\nu F_\nu^{\rm pk} \propto \nu_{\rm pk}^2$.

Therefore, we conclude that the synchrotron peak shift found in our data set is consistent with the variability being dominated by a changing magnetic field. However, as pointed out above, we need to caution that such a change in the magnetic field might realistically also impact the shape of the electron distribution, primarily through a changing synchrotron cooling time scale. Clearly, more sophisticated analyses of this synchrotron peak shift are needed, but are beyond the scope of this paper.

We note that the shape of the optical SEDs found in all of our observations contradicts the optical-UV spectrum observed by Swift/UVOT on 2008 May 2 and 8, which indicates a rising slope throughout the optical regime (Abdo et al. 2010). However, most of our observations were taken during moderately faint states of the source, while the Swift/UVOT spectrum corresponds to a bright state, similar to the major optical flare that triggered the MAGIC detection in 2007. Given the trend of the synchrotron peak shift which we found in our data, it is conceivable that the Swift/UVOT observations correspond to an extreme case of a high synchrotron peak frequency, in accord with a very high optical flux.

This work was supported by NASA through Chandra Guest Observer Program award GO8-9100X, XMM-Newton Guest Observer Program awards NNX08AD67G and NNX09AV45G, and Fermi Guest Investigator Program award NNX09AT82G.

REFERENCES

Abdo, A. A., et al., 2010, ApJ, 716, 30

Aharonian, F., et al., 2007, ApJ, 664, L71

Albert, J., et al., 2007a, ApJ, 669, 862

Albert, J., et al., 2007b, ApJ, 667, L21

Böttcher, M., 2007, ApSS, 309, 95

Dwek, E., & Krennrich, F., 2005, apJ, 618, 657

Edelson, R. A., & Krolik, J. H., 1988, ApJ, 333, 646

Elvis, M., Plummer, D., Schachter, J., & Fabbiano, G., 1992, ApJS, 80, 257

Finke, J. D., Razzaque, S., & Dermer, C. D., 2010, ApJ, 712, 238

Franceschini, A., Rodighiero, G., & Vaccari, M., 2008, A&A, 487, 837

Gilmore, R. C., et al., 2009, MNRAS, 399, 1694

Hartman, R. C., et al., 1999, ApJS, 129, 79

Landoldt, A. U., 1992, AJ, 104, 340

Massey, P., & Davis, L. E., 1992, "A User's Guide to Stellar CCD Photometry with IRAF", `http://iraf.net/irafdocs/daophot2/`

Mücke, A., & Protheroe, R. J., 2001, Astropart. Phys., 15, 121

Mücke, A., Protheroe, R. J., Engel, R., Rachen, J. P., & Stanev, T., 2003, Astropart. Phys., 18, 593

Raiteri, C. M., et al., 2008, A&A, 491, 755

Sowards-Emmerd, D., Roman, R. W., & Michelson, P. F., 2003, ApJ, 590, 109

Stecker, F. W., Malkan, M. A., & Scully, S. T., 2006, ApJ, 648, 774